



**GEOLOGICAL SURVEY OF CANADA
OPEN FILE 7853**

Targeted Geoscience Initiative 4: Contributions to the Understanding of Volcanogenic Massive Sulphide Deposit Genesis and Exploration Methods Development

Hyperspectral reflectance spectrometry in the exploration for VMS deposits using the Izok Lake Zn-Cu-Pb-Ag deposit, Nunavut as a test site

Kati Laakso¹, Benoit Rivard¹, and Jan M. Peter²

¹University of Alberta, Edmonton, Alberta

²Geological Survey of Canada, Ottawa, Ontario

2015

© Her Majesty the Queen in Right of Canada, as represented by the Minister of Natural Resources Canada, 2015

This publication is available for free download through GEOSCAN (<http://geoscan.nrcan.gc.ca/>)

Recommended citation

Laakso, K., Rivard, B., and Peter, J.M., 2015. Hyperspectral reflectance spectrometry in the exploration for VMS deposits using the Izok Lake Zn-Cu-Pb-Ag deposit, Nunavut as a test site, *In: Targeted Geoscience Initiative 4: Contributions to the Understanding of Volcanogenic Massive Sulphide Deposit Genesis and Exploration Methods Development*, (ed.) J.M. Peter and P. Mercier-Langevin; Geological Survey of Canada, Open File 7853, p. 15–25.

Publications in this series have not been edited; they are released as submitted by the author.

Contribution to the Geological Survey of Canada's Targeted Geoscience Initiative 4 (TGI-4) Program (2010–2015)

TABLE OF CONTENTS

Abstract	17
Introduction	17
Sampling Methods	19
Ground Spectrometry	19
Laboratory Spectrometry	19
Lithogeochemistry	19
Airborne Spectrometry	20
Results	20
Spatial Distribution of the Ground and Laboratory Absorption Feature Wavelength Positions	20
Alteration Intensity Variation Extracted from the Alteration Indices	21
Discussion	23
Implications for Exploration	23
Acknowledgements	24
References	24
Figures	
Figure 1. Locational and geological map of the study area showing the locations of the ground spectrometric data and drill-core sites	18
Figure 2. Ground reflectance spectra and hull quotient-corrected spectra for measurements 313 and 134	21
Figure 3. Colour ramp map of the interpolated Al-OH absorption feature wavelengths extracted from the ground spectrometry	21
Figure 4. Colour ramp map of the interpolated Fe-OH absorption feature wavelengths extracted from the ground spectrometry	21
Figure 5. Bivariate plots of Al-OH and Fe-OH absorption feature wavelength positions of the ground and drill-core spectra versus distance from massive sulphide mineralization	22
Figure 6. Colour ramp map of the AI and symbol map of the alteration box plot results	22
Figure 7. Colour ramp map of the interpolated Al-OH absorption feature wavelengths extracted from the airborne data	23

Hyperspectral reflectance spectrometry in the exploration for VMS deposits using the Izok Lake Zn-Cu-Pb-Ag deposit, Nunavut as a test site

Kati Laakso^{1*}, Benoit Rivard¹, and Jan M. Peter²

¹Centre for Earth Observation Sciences at the University of Alberta, Department of Earth and Atmospheric Sciences, University of Alberta, 1-26 Earth Sciences Building, University of Alberta, Edmonton, Alberta T6G 2E3

²Central Canada Division, Geological Survey of Canada, 601 Booth Street, Ottawa, Ontario K1A 0E8

*Corresponding author's e-mail: laakso@ualberta.ca

ABSTRACT

We have investigated the application of ground, laboratory and airborne optical remote sensing methods to the detection of hydrothermal alteration zones associated with volcanogenic massive sulphide (VMS) deposits using the Izok Lake Zn-Cu-Pb-Ag deposit, Nunavut as a test site. The deposit is located in a sub-arctic environment where lichens are abundant on the rock outcrops. The rhyolitic host rocks to the deposit have been hydrothermally altered and contain white mica and chlorite group minerals. These alteration minerals have Al-OH and Fe-OH absorption features in the short-wave infrared (SWIR) wavelength region. The absorption feature wavelength positions can shift as a function of chemical compositional changes within minerals. In and around the Izok Lake deposit there are systematic trends in the Al-OH and Fe-OH absorption feature wavelength positions with distance from the massive sulphide lenses. Furthermore, these trends can be detected in bulk rock lithogeochemical data. Our results demonstrate the feasibility of using hyperspectral remotely sensed data to delineate hydrothermal alteration zones and determine alteration intensity in high-latitude regions.

INTRODUCTION

Volcanogenic massive sulphide (VMS) deposits are economically important sources of metals (Gibson et al., 2007) formed on or near the seafloor from hydrothermal systems that are spatially and temporally associated with submarine magmatism and volcanism. Cold seawater is drawn into the upper parts of the crust, which results in the establishment of a convective cell of circulating hydrothermal fluids. As the fluid temperature increases, metals are leached from the host rocks. These dissolved metals are precipitated near the seafloor, resulting in the formation of massive sulphide lenses. A key geochemical reaction along the fluid flow path is the breakdown of feldspar minerals through interactions with acidic hydrothermal fluids, and the subsequent formation of white micas and chlorite (Barrett and MacLean, 1994). The temperature and chemical gradients induced by mixing of high-temperature hydrothermal fluids with cold seawater result in a range of chemical, mineralogical and textural changes in the host rocks and the precipitation of syngenetic and stratabound accumulations of massive to semi-massive sulphides. These phyllosilicates are typical hydrothermal alteration minerals. Generally, the stratigraphic footwall immediately beneath the massive sul-

phides is characterized by chloritic alteration, and the areas more distal from the massive sulphides by sericitic alteration.

The white mica group minerals formed during VMS-associated hydrothermal alteration can have variable chemical compositions that range from paragonite to muscovite to celadonite. Paragonite is favoured at high temperatures (Duke, 1994), but the chemical composition of the hydrothermal fluids and the water/rock ratio of the system may also simultaneously influence the composition (Kranidiotis and MacLean, 1987). The chemical composition of the phyllosilicate minerals may be governed through Tschermak substitution, in which tetrahedral Si substitution for Al is coupled with octahedral Mg-Fe substitution for Al. These substitutions can be observed as spectral shifts within the Al-OH absorption features near 2200 nm (Bishop et al., 2008). The wavelength position of this absorption feature shifts systematically toward shorter wavelengths as the Al content of the octahedral sites increases, and a systematic shift toward longer wavelengths takes place when the relative proportion of octahedral Mg and Fe increase (Duke, 1994). Similar changes take place in the chlorite group minerals that show a spectral shift of an Fe-OH absorption feature near 2250 nm

Laakso, K., Rivard, B., and Peter, J.M., 2015. Hyperspectral reflectance spectrometry in the exploration for VMS deposits using the Izok Lake Zn-Cu-Pb-Ag deposit, Nunavut as a test site, *In: Targeted Geoscience Initiative 4: Contributions to the Understanding of Volcanogenic Massive Sulphide Deposit Genesis and Exploration Methods Development*, (ed.) J.M. Peter and P. Mercier-Langevin; Geological Survey of Canada, Open File 7853, p. 15–25.

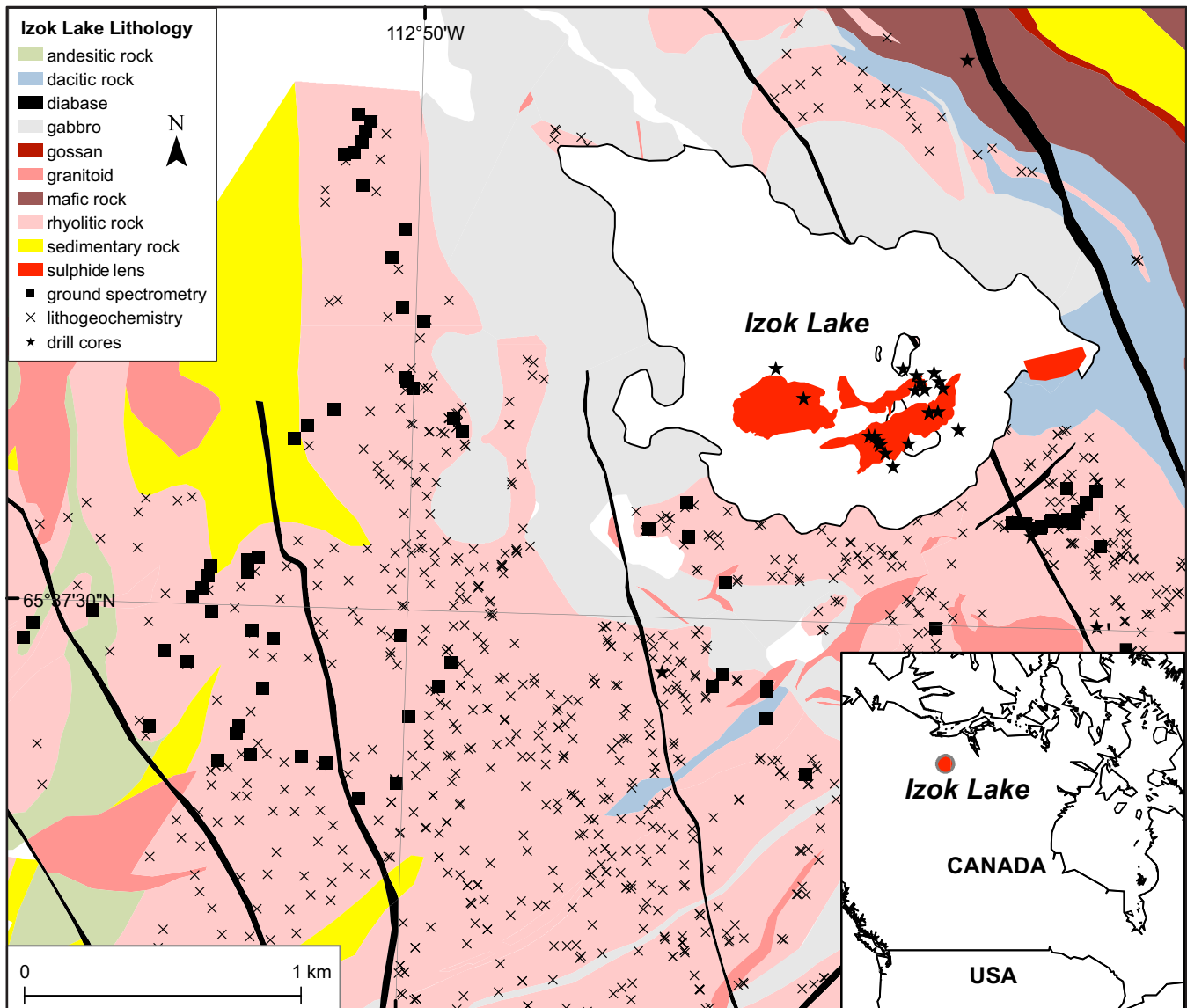


Figure 1. Locational (inset) and geological map of the study area showing the locations of the ground spectrometric data (black squares) and drill-core sites (stars). The airborne survey covers the whole study area. The geology, surface projections of sulphide lenses on islands and under Izok Lake and locations of lithochemical samples (x) are from MMG Ltd. (unpubl.).

toward shorter wavelengths with increasing Mg, and toward longer wavelengths with increasing Fe (McLeod et al., 1987).

Several hydrothermal alteration indices have been developed to determine alteration style and measure its intensity (e.g. Ishikawa et al., 1976; and references therein). These indices are calculated using elements that were added (numerator) and those that were lost (denominator) during alteration. The spatial distribution of the alteration index values can then be used to vector toward massive sulphide mineralization.

Our study area is the Izok Lake Zn-Cu-Pb-Ag VMS deposit which is located at 65°38'N, 112°48'W in the Point Lake greenstone belt, Nunavut (Fig. 1). The deposit is comprised of several massive sulphide lenses that are hosted by rhyolitic rocks. These rocks contain

white mica and chlorite group minerals that result from hydrothermal alteration during massive sulphide formation (Morrison, 2004), and here we present spectral and bulk geochemical data for these rhyolitic rocks. The Izok Lake region is characterized by Arctic tundra vegetation that is dominated by shrubs, sedges, grasses and flowering herbs (Laidler et al., 2008), and many rock outcrops in the study area are covered by abundant lichens. These lichens mask the spectral characteristics of the rocks, potentially compromising the use of remote sensing data for geologic applications. A comprehensive description of the study area is given in Laakso et al. (in press).

The research objective was to assess the applicability of hyperspectral remote sensing to the detection and delineation of hydrothermal alteration zones associated

with the Izok Lake deposit. White micas, biotite and chlorite are the predominant phyllosilicate alteration minerals near the Izok Lake deposit, and for this reason, the Al-OH and Fe-OH absorption feature wavelengths positions were measured using ground, laboratory and airborne hyperspectral instruments. The ground data were also compared with hydrothermal alteration indices calculated from bulk lithogeochemical data to determine if the spectral data could serve as a proxy for mapping hydrothermal alteration.

SAMPLING AND METHODS

Ground Spectrometry

These data were acquired throughout the study area with the objective of mapping any outcropping hydrothermal alteration zones associated with the Izok Lake deposit. A total of 285 spectra were acquired from the areas in the vicinity of the massive sulphide mineralization. At each rock outcrop, one to eight spectral measurements, each with a 1 cm diameter circular outline, were collected from lichen-free weathered rock surfaces. The spectra were acquired with an ASD FieldSpec[®] Pro 3 spectrometer that records in the 350–2500 nm wavelength range with a spectral resolution of 10 nm in the short-wave infrared wavelength region. The spectrometer was equipped with a fore optic contact probe to ensure consistent illumination conditions during data acquisition. Radiance values were converted to reflectance values by means of a panel of pressed polytetrafluoroethylene, commercially known as Spectralon[™] (Labsphere, New Hampshire, US). The geographic coordinates of the field sites were recorded with a handheld GPS.

The Al-OH and Fe-OH absorption feature wavelength positions of the spectra were extracted to discern any spectral shifts associated with the areas of hydrothermally altered rock. An average wavelength position was then computed from these spectra; this was achieved by conducting continuum removal and recording the minimum (the smallest hull quotient value) of each spectrum. Next, these values were averaged per rock outcrop, and this resulted in 98 Al-OH and 85 Fe-OH absorption feature wavelength position observations (Fig. 1). The inverse distance weighting (IDW: ArcGIS Desktop: Release 10, Environmental Systems Research Institute) interpolation technique was used to create a continuous surface of the Al-OH and Fe-OH wavelength positions. The results were clipped to a 200 m radius around each averaged ground spectrum to minimize extrapolation and to create a realistic representation of the spatial trends of the absorption feature wavelength positions of the study area.

In a separate analysis, the horizontal distance between each spectral result at the measurement loca-

tions and its nearest massive sulphide lens (see Fig. 1) was calculated to investigate the spectral trends as a function of distance from the massive sulphide lenses.

Laboratory Spectrometry

In order to establish the character and extent of the hydrothermal alteration zones of the Izok Lake deposit in the vertical dimension, spectrometric data were obtained from 28 drill cores (Fig. 1). Of the 781 spectral readings that were acquired with an ASD FieldSpec 3 spectrometer and a TerraSpec 4 hi-resolution mineral spectrometer, 624 spectra were from rhyolitic rocks. The measurements obtained from the rhyolitic rocks were calibrated to reflectance and the Al-OH and Fe-OH wavelength positions of each measurement were extracted as described above for ground spectral measurements.

The distance between each Al-OH and Fe-OH absorption feature observations of the drill cores and its spatially nearest massive sulphide lens was calculated to investigate changes in the spectral properties of the phyllosilicate minerals with distance to the mineralization. The locations and spatial dimensions of the massive sulphide lenses were extracted from the drill-core logs of MMG Ltd. Finally, the results obtained from the drill-core spectra were combined with the corresponding ground spectral results to obtain a three-dimensional model of the spatial variation of the Al-OH and Fe-OH absorption feature wavelength positions in the Izok Lake deposit.

Lithogeochemistry

A database of whole-rock major element oxide analyses of 2902 rock outcrop hand samples collected from the study area was provided by MMG Ltd. (Fig. 1). These samples are from areas proximal and distal to mineralization. The locations of the samples are shown in Figure 1. Whole-rock major oxide analyses were performed by ALS Minerals (North Vancouver, B.C.) using Inductively Coupled Plasma-Atomic Emission Spectroscopy (ICP-AES) on rock powders.

A subset of the database that encompasses 1241 rhyolitic rock samples was used to identify large-scale hydrothermal alteration trends across the study area. Hydrothermal alteration was assessed by means of the Ishikawa index (AI: Ishikawa et al., 1976):

$$AI = 100(K_2O + MgO) / (K_2O + MgO + Na_2O + CaO)$$

The IDW interpolation technique was used to create a continuous representation of the AI values across the study area.

The AI has two drawbacks for quantifying hydrothermal alteration. First, it does not take into account carbonate alteration that can be significant in some VMS deposits. Second, it does not differentiate

between sericitic and chloritic alteration. For these reasons, Large et al. (2001) introduced the Chlorite-Carbonate-Pyrite Index (CCPI):

$$\text{CCPI} = 100(\text{FeO} + \text{MgO}) / (\text{FeO} + \text{MgO} + \text{Na}_2\text{O} + \text{K}_2\text{O})$$

The Alteration Box Plot (Large et al., 2001) plots the AI values against the CCPI values to discern different alteration trends within VMS deposits. Here, we use the Alteration Box Plot to account for possibly distinct hydrothermal alteration zones in the study area and summarize the results (AI+CCPI) to determine the spatial distribution of these zones. Furthermore, the alteration intensity estimates are divided into four quartiles that each represent a fourth of the sampled population. The results were spatially joined with their nearest Al-OH wavelength position to assess the capability to infer alteration intensity estimates from hyperspectral remote sensing data.

Airborne Spectrometry

Airborne hyperspectral data were acquired over a 94 km² area comprising 58 flight lines within the Point Lake greenstone belt in August, 2010. The data were acquired by SpecTIR LLC (Reno, Nevada) using the ProSpecTIR[®] (AISA dual) sensor at a spatial resolution of 1 m. This sensor collects data in a nominal spectral resolution of 5 nm between 390 to 2500 nm. These data were resampled to a 6.3 nm interval, resulting in 360 spectral channels.

The airborne dataset was pre-processed by SpecTIR by first radiometrically calibrating the digital numbers of the raw data to radiance values using the preflight gains and offsets measured by the sensor manufacturer. Next, the radiance data was atmospherically corrected to reflectance data using the ATCOR-4[®] software package (Richter and Schläpfer, 2002). Finally, the dataset was geospatially corrected using the data extracted from a three-axis gyroscope attitude INS (Inertial Navigation System) that was positioned with a 12-channel GPS system.

The airborne data were analyzed and compared with the ground spectral dataset to investigate the accuracy of the Al-OH absorption feature wavelength positions extracted from the airborne dataset. First, pixels in the airborne data associated with vegetation were removed by means of the Normalized Difference Vegetation Index (NDVI₇₀₅; Gitelson and Merzlyak, 1994) to which a threshold was applied. Next, spectral endmembers were extracted from the remaining pixels using the Spatial-Spectral Endmember Extraction (SSEE) tool of Rogge et al. (2007). Of the 137 endmembers extracted, 22 were selected to represent rocks, vegetation and lichens, or mixtures of these. This endmember spectral database was then input into the linear spectral unmixing computer calculations.

The resulting endmember images were investigated and a single endmember image was chosen to represent pixels of the rhyolitic rock outcrops with a minimal lichen cover. A threshold was extracted from this image and applied to the original hyperspectral image to retain rhyolitic rock outcrop pixels with sparse vegetation and the lowest degree of lichen cover.

Next, the wavelength position of the Al-OH absorption feature was calculated after hull removal from the 2188–2212 nm wavelength range. Wavelength positions at 2194 nm and 2212 nm were discarded because they are likely associated with vegetation rather than the rhyolitic rocks, and hence only the wavelengths at 2200 nm and 2206 nm were used in the airborne data analysis. At this stage, 261 pixels remained, representing <1% of the original amount of pixels associated with the rhyolitic rock outcrops in the airborne data. As with the ground spectral and lithochemical datasets, an interpolated surface was created from the result using the IDW tools of the ArcGIS software package. The result was cropped to a 200 m diameter buffer around each observation in order to minimize the effects of extrapolation to areas of no observations. This protocol was not repeated for the Fe-OH absorption features of biotite/chlorite because these minerals could not be reliably detected in the airborne hyperspectral dataset.

The results were then compared with the ground spectral dataset. This dataset was resampled from the sampling interval of the ground spectrometry (1 nm in the SWIR wavelength region) to the sampling interval of the airborne spectrometry (6.3 nm). The Al-OH absorption feature wavelength positions (n=261) of the airborne spectrometric dataset were then linked with their geographically nearest Al-OH absorption feature wavelength positions of the ground spectral dataset. The accuracy of the airborne result was assessed by calculating the differences between the Al-OH absorption feature wavelength positions of the airborne and ground spectral datasets.

RESULTS

Spatial Distribution of the Ground and Laboratory Absorption Feature Wavelength Positions

An Al-OH absorption feature is present in >90% of the rhyolitic rock outcrops, indicating that the mineral responsible for this spectral feature is ubiquitously abundant throughout the study area. The average wavelengths of the absorption features in these outcrops varies between 2194 and 2211 nm. The wide range of the absorption feature wavelengths results from spectral shifts, as is illustrated in Figure 2a and b. The spatial distribution of the Al-OH absorption features of the

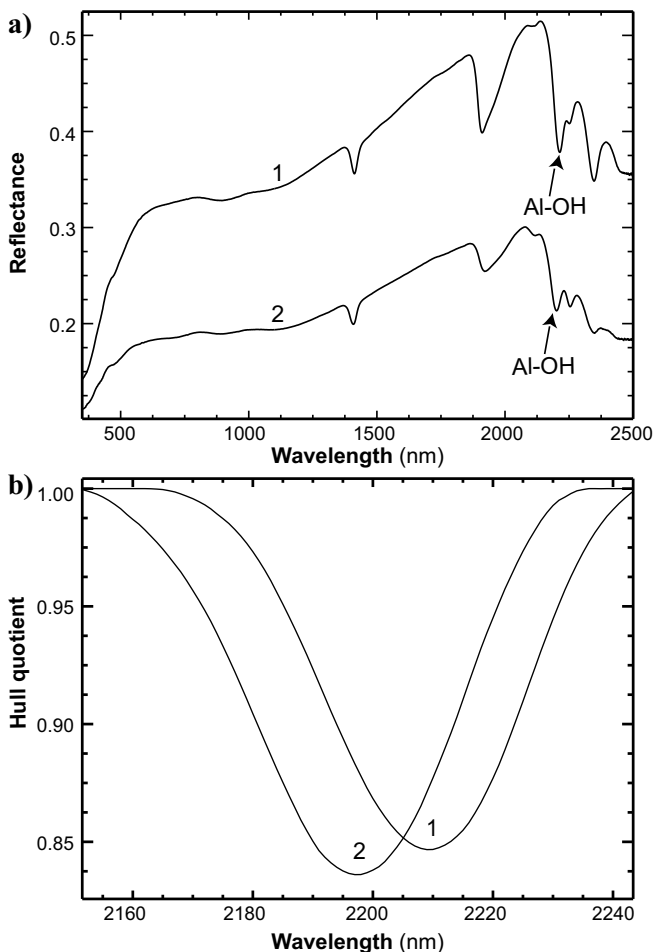


Figure 2. a) Ground reflectance spectra for measurement 313 (2211 nm, spectrum 1) and 134 (2197 nm, spectrum 2); b) hull quotient-corrected spectra 1 and 2 shown in (a).

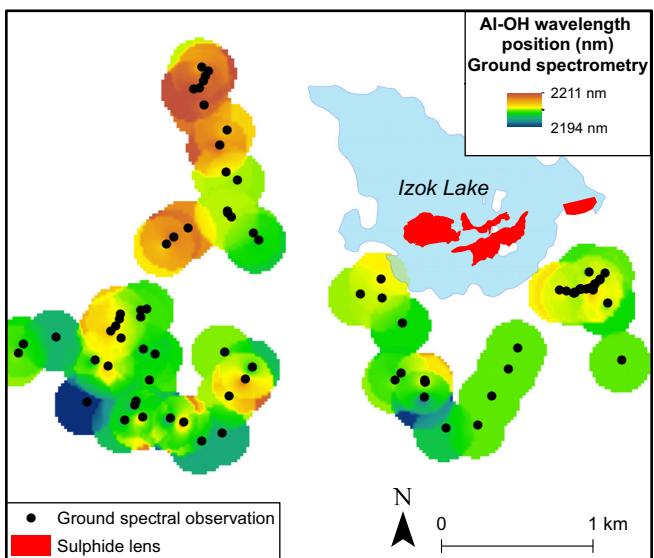


Figure 3. Colour ramp map of the interpolated Al-OH absorption feature wavelengths extracted from the ground spectrometry, the geographic data and surface projections of the sulphide lenses are from MMG Ltd. (unpubl.).

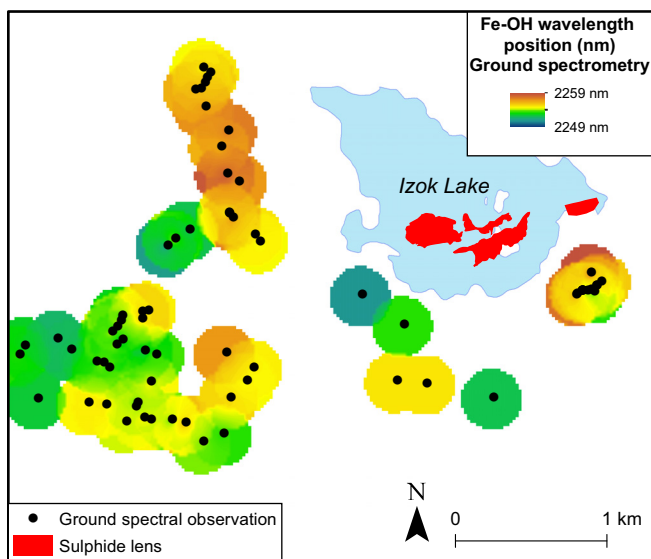


Figure 4. Colour ramp map of the interpolated Fe-OH absorption feature wavelengths extracted from the ground spectrometry; the geographic data and surface projections of the sulphide lenses are from MMG Ltd. (unpubl.).

ground spectral dataset, shown in Figure 3, suggests that the rocks surrounding the massive sulphide lenses contain relatively long Al-OH absorption feature wavelengths, with the highest Al-OH absorption features located northwest of the massive sulphide lenses.

An Fe-OH absorption was observed in 79% of the rock outcrops, indicating that this mineral group is less common than white micas in the study area. The average Fe-OH wavelengths of the rock outcrops range between 2249 and 2259 nm. The spatial distribution of the Fe-OH absorption features suggest that the longest Fe-OH absorption feature wavelength positions occur near the massive sulphide lenses (Fig. 4).

The spatial distributions of the Al-OH and Fe-OH absorption feature wavelength positions extracted from both the ground and drill-core spectra were further assessed by correlating them with their distance to the nearest massive sulphide mineralization. The results, shown in Figure 5a and b, indicate that rocks within 500 m of massive sulphide mineralization display considerable variation in the Al-OH and Fe-OH wavelength positions. Moreover, the shift toward longer Al-OH and Fe-OH absorption feature wavelength positions can be observed approximately 1000 to 2000 m from the massive sulphide lenses. It is notable that this trend is more evident in the Fe-OH absorption features than in the Al-OH absorption features that show weak or non-existent trends in the study area.

Alteration Intensity Variation Extracted from the Alteration Indices

Figure 6 show the spatial distribution of the AI and the Alteration Box plot values. This figure indicates that

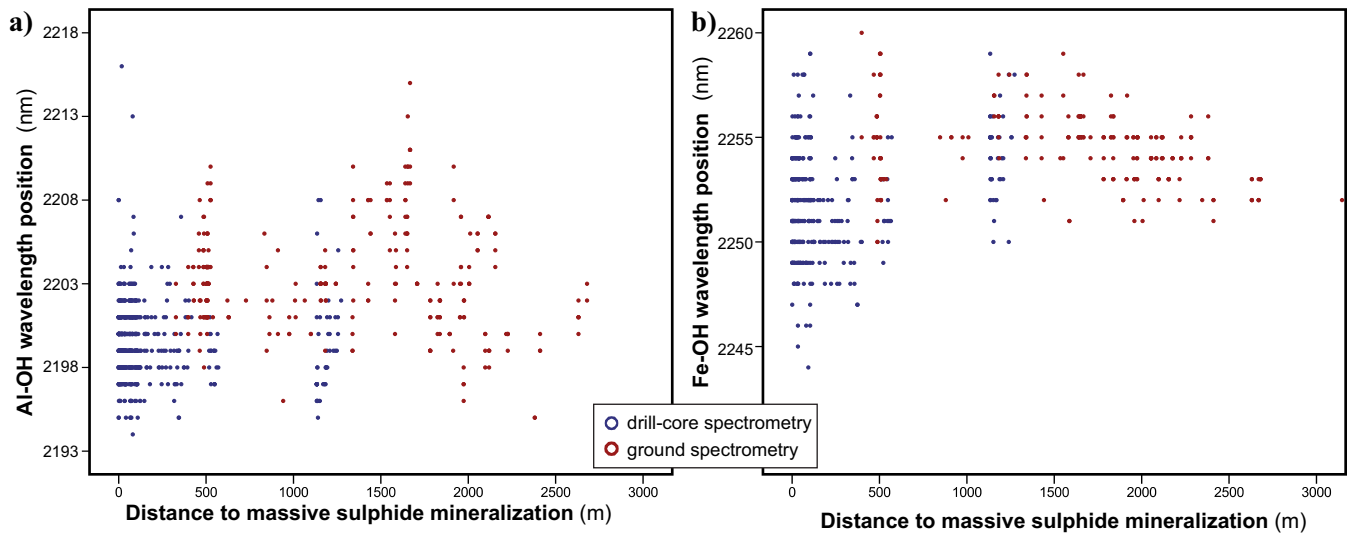


Figure 5. Bivariate plots of (a) Al-OH absorption feature wavelength positions of the ground and drill-core spectra versus distance from massive sulphide mineralization; and (b) Fe-OH absorption feature wavelength positions of the ground and drill-core spectra versus distance from massive sulphide mineralization. The results are shown for the intensely altered area within a 3000 m diameter distance of the deposit.

the rhyolitic rocks around the massive sulphide lenses have been intensely altered, as evidenced by high (99%) alteration intensity values. Moreover, both alteration intensity estimates show an area of intense hydrothermal alteration that spans up to 2.7 km southwest from the massive sulphide lenses (Fig. 6a,b). The high AI values of this area suggest near complete replacement of feldspars and glass by white mica and chlorite (Large et al., 2001).

The correlation between the alteration intensity and the Al-OH absorption feature in the ground spectra was

investigated using Pearson product-moment correlation coefficient analysis. This was done by calculating the correlation coefficient between the Al-OH absorption feature wavelength positions of the ground spectral dataset and the Alteration Box Plot values subdivided into quartile ranges. The results (Fig. 6b) show a moderate, inverse correlation ($r=-0.486$, $n=85$, 99% confidence level, two-tailed) between these datasets, indicating that high alteration intensities are associated with a shift toward shorter Al-OH absorption feature wavelength positions.

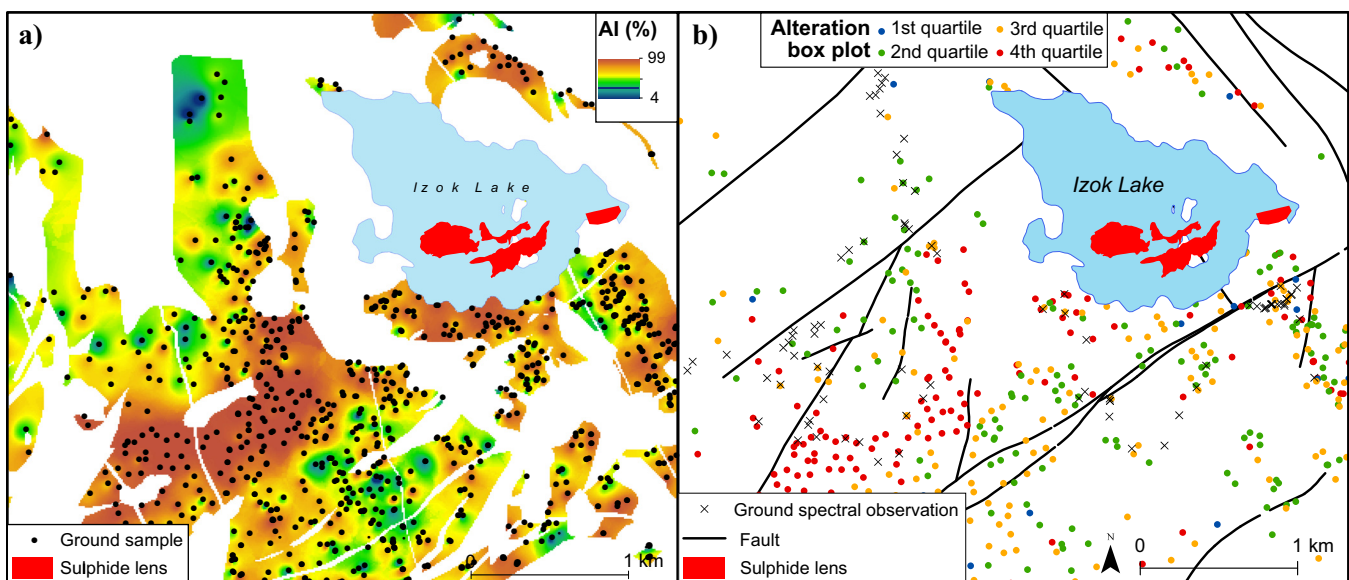


Figure 6. a) Colour ramp map of the AI content (%). b) Symbol map of the alteration box plot results, divided into four quartiles. Also shown are the measurement locations of the Al-OH absorption feature wavelength positions in the ground spectral dataset. The plot displays the AI and CCPI values of each lithogeochemical sample summarized and divided into four quartiles.

Airborne Spectrometric Absorption Feature Wavelengths

The Al-OH absorption feature wavelength positions of the airborne data (n=261) show a bimodal frequency distribution with absorption features at 2200 nm and at 2206 nm. A comparison between the ground and airborne spectral datasets reveals a relatively low accuracy of the airborne spectrometry as measured by the difference between the ground and airborne spectra: 65% of the Al-OH absorption feature wavelength positions of the airborne data (n=169) are within three nanometres of their spatially nearest airborne spectrometric value. However, in the vicinity of the massive sulphide lenses there is a zone of relatively long Al-OH absorption feature wavelength positions, spanning between 2200 and 2206 nm. This area coincides spatially with the relatively long Al-OH absorption feature wavelength positions in the ground spectrometric data that range between 2197 and 2211 nm. This area, located 800 to 1900 m west of the sulphide lenses coincides spatially with a high alteration intensity area (Figs. 6b, 7). Previous studies have suggested that phengitic white micas preferably develop in areas of high-temperature fluid flow (e.g. Hellyer VMS deposit; Yang et al., 2011).

DISCUSSION

There is considerable variation in the Al-OH absorption feature wavelength positions of white micas in the Izok Lake area indicative of variable effects of hydrothermal alteration processes. The Al-OH wavelength range of the ground spectral dataset (2194–2211 nm) suggests that the chemical composition of white micas ranges from paragonitic to muscovitic to slightly phengitic. Similarly, the Fe-OH wavelength range of biotite/chlorite (2249–2259 nm) indicates that these minerals have Mg-rich, intermediate and Fe-rich compositions in the study area. Iron enrichment is common in the highly altered areas of VMS deposits that typically contain Fe-rich chlorite (e.g. MacLean and Hoy, 1991) and hence iron enrichment near the massive sulphide lenses conforms to this idealized model. Both the white micas and biotite/chlorite show strongest variation in the Al-OH and Fe-OH absorption feature wavelength positions in the immediate vicinity (0–500 m) of the massive sulphide lenses (Fig. 5), indicative of strong temperature and geochemical gradients at the time of massive sulphide formation.

The alteration intensity variation of the Izok Lake area was estimated by means of the AI and the alteration box plot. Correlations between the alteration box plot and the Al-OH absorption feature wavelength positions reveal a relationship between high alteration intensity values and a shift toward shorter Al-OH absorption feature wavelength positions. Nevertheless,

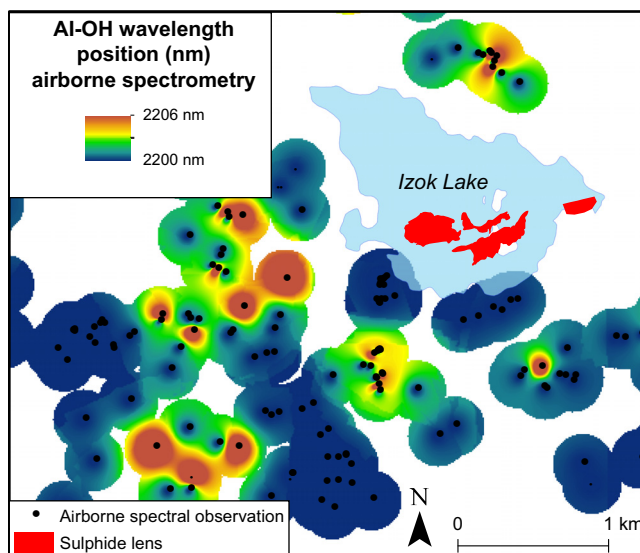


Figure 7. Colour ramp map of the interpolated Al-OH absorption feature wavelengths extracted from the airborne data; the surface projection of the sulphide lenses is from MMG Ltd. (unpubl.).

the area of high alteration intensities (800 to 1900 m from the massive sulphide lenses) is characterized by relatively long Al-OH absorption feature wavelength positions (up to 2211 nm), and hence the shift toward shorter wavelengths is relative. Also, there is no one-to-one correspondence between the hyperspectral datasets and the lithogeochemical data.

A comparison between the airborne and ground spectra reveals a detection accuracy of 65%. This low accuracy of the airborne spectrometric data may result from the abundant lichen cover that necessitated the masking out of 99% of the pixels associated with the rhyolitic rock outcrops. Contrary to the white mica group minerals, the Fe-OH absorption features of biotite/chlorite group minerals could not be detected in the airborne hyperspectral dataset. One factor that may have contributed to this result is the lower abundance of these minerals in the study area: white micas were observed in >90% of the rhyolitic rock outcrops, whereas biotite/chlorite group minerals were observed in only 79% of the rhyolitic rock outcrops.

Despite the relatively low detection accuracy of the airborne spectrometric data, the ability to detect an area of phengitic muscovite using both the ground and airborne datasets independently demonstrates the efficacy of airborne spectrometry for the recognition and delineation of zones of hydrothermally altered rocks in outcrops in the Izok Lake area.

IMPLICATIONS FOR EXPLORATION

Our results indicate that hydrothermal alteration zones associated with VMS deposits can be detected by ground and airborne hyperspectral remote sensing of

natural outcrops, despite the presence of abundant lichen cover. Given the similarity in alteration styles between VMS and orogenic gold deposits, the method has applicability to such deposits, and likely other styles of mineralization that have pronounced associated alteration zones.

Our study highlights the importance of careful selection of wavelengths for image analysis in environments where the spectral signatures are strongly influenced by spectral mixing between two or several elements. Two absorption feature wavelength positions (2194 nm and 2212 nm) were discarded from the airborne dataset due to the effects of spectral mixing of rocks and vegetation that could not be completely eliminated through spectral unmixing analysis.

Airborne surveying of prospective areas (e.g. greenstone belts) may provide a relatively low cost, “green” (i.e. no ground disturbance) mineral exploration method that can be utilized in conjunction with other traditional methods. Optical remote sensing methods are likely to be increasingly used in exploration in Canada’s sparsely vegetated north given the impending availability of (albeit lower spatial resolution) commercial satellite and microsatellite hyperspectral sensors that are soon to be launched by several countries (see e.g. Staenz et al., 2013). The hyperspectral detection of hydrothermal alteration zones in remote, high-latitude regions of Canada (and elsewhere) that typically lack infrastructure may provide a facile and cost-effective exploration method to augment traditional geological, geochemical, and geophysical methods. Our study lends support for the development of future airborne and spaceborne hyperspectral sensors of higher spectral resolutions that would allow for better spectral unmixing and separation of cellulose and non-photosynthetic vegetation materials from white mica and chlorite group minerals. Unmanned Aerial Vehicles (UAVs) may also be a platform that can provide valuable high spatial resolution hyperspectral data at the regional scale.

ACKNOWLEDGMENTS

Funding came from the Research Affiliate Program and a grant from the Targeted Geoscience Initiative 4 (TGI-4) Program of the Earth Sciences Sector, Natural Resources Canada. The hyperspectral airborne data were acquired under the Strategic Investment in Northern Economic Development (SINED) Program of Indian and Northern Affairs Canada (now Aboriginal and Northern Affairs Canada), and we gratefully acknowledge the contributions of Donald James in facilitating the survey. We thank MMG Ltd., particularly Kimberley Bailey, Trish Toole, Ian Neill, and Dave Kelley, for logistical and field support in 2010 and 2013, and for geological discussions and

access to company data. A review by Jeanne Percival (Geological Survey of Canada) helped to clarify the text.

REFERENCES

- Barrett, T.J. and MacLean, W.H., 1994. Mass changes in hydrothermal alteration zones associated with VMS deposits of the Noranda area; *Exploration and Mining Geology*, v. 3, p. 131–160.
- Bishop, J.L., Lane, M.D., Dyar, M.D., and Brown, A.J., 2008. Reflectance and emission spectroscopy study of four groups of phyllosilicates: smectites, kaolinite-serpentinates, chlorites and micas; *Clay Minerals*, v. 43, p. 35–54.
- Duke, E.F., 1994. Near infrared spectra of muscovite, Tschermak substitution, and metamorphic reaction progress: Implications for remote sensing; *Geology*, v. 22, p. 621–624.
- Gibson, H.L., Allen, R.L., Riverin, G. and Lane, T.E., 2007. The VMS model: Advances and application to exploration geology, *In: Proceedings of Exploration 07*, (ed.) B. Milkereit; Fifth Decennial International Conference on Mineral Exploration, Toronto, September 9-12, 2007, p. 713–730.
- Gitelson, A. and Merzlyak, M.N., 1994. Spectral reflectance changes associated with autumn senescence of *Aesculus hippocastanum* L. and *Acer platanoides* L. leaves. Spectral features and relation to chlorophyll estimation; *Journal of Plant Physiology*, v. 143, p. 286–292.
- Ishikawa, Y., Sawaguchi, T., Iwaya, S.-I. and Horiuchi, M., 1976. Delineation of prospecting targets for Kuroko deposits based on modes of volcanism of underlying dacite and alteration haloes; *Mining Geology*, v. 26, p. 105–117.
- Kranidiotis, P. and MacLean, W., 1987. Systematics of chlorite alteration at the Phelps Dodge massive sulfide deposit, Matagami, Quebec; *Economic Geology*, v. 82, p. 1898–1911.
- Laakso, K., Rivard, B., Peter, J., White, H., Maloley, M., Harris, J. and Rogge, D., in press. Application of airborne, laboratory and field hyperspectral methods to mineral exploration in the Canadian Arctic: recognition and characterization of volcanogenic massive sulfide-associated hydrothermal alteration in the Izok Lake deposit area, Nunavut, Canada; *Economic Geology*.
- Laidler, G.J., Treitz, P.M., and Atkinson, D.M., 2008. Remote sensing of Arctic vegetation: Relations between the NDVI, spatial resolution and vegetation cover on Boothia Peninsula, Nunavut; *Arctic*, v. 61, p. 1–13.
- Large, R.R., Gemmell, J.B., Paulick, H., and Huston, D.L., 2001. The alteration box plot: A simple approach to understanding the relationship between alteration mineralogy and lithochemistry associated with volcanic-hosted massive sulfide deposits; *Economic Geology*, v. 96, p. 957–971.
- MacLean, W. and Hoy, L.D. 1991. Geochemistry of hydrothermally altered rocks at the Horne Mine, Noranda, Quebec; *Economic Geology*, v. 86, p. 506–528.
- McLeod, R.L., Gabell, A.R., Green, A.A., and Gardavsky, V., 1987. Chlorite infrared spectral data as proximity indicators of volcanogenic massive sulphide mineralisation, *In: Proceedings; Pacific Rim Congress ‘87*, Gold Coast, Australia, August 26–29, 1987, p. 321–324.
- Morrison, I.R., 2004. Geology of the Izok massive sulfide deposit, Nunavut Territory, Canada; *Exploration and Mining Geology*, v. 13, p. 25–36.
- Richter, R. and Schläpfer, D., 2002. Geo-atmospheric processing of airborne imaging spectrometry data. Part 2: Atmospheric/topographic correction; *International Journal of Remote Sensing*, v. 23, p. 2631–2649.

Hyperspectral reflectance spectrometry in the exploration for VMS deposits using the Izok Lake deposit as a test site

- Rogge, D.M., Rivard, B., Zhang, J., Sanchez, A., Harris, J., and Feng, J., 2007. Integration of spatial-spectral information for the improved extraction of endmembers; *Remote Sensing of Environment*, v. 110, p. 287–303.
- Staenz, K., Mueller, A., and Heiden, U., 2013. Overview of terrestrial imaging spectroscopy mission, In: *Transactions of 2013 IEEE International Geoscience and Remote Sensing Symposium (IGARSS)*, Melbourne, Australia, July 21-26, 2013, p. 3502–3505.
- Yang, K., Huntington, J.F., Gemmill, J.B., and Scott, K.M., 2011. Variations in composition and abundance of white mica in the hydrothermal alteration system at Hellyer, Tasmania, as revealed by infrared reflectance spectroscopy; *Journal of Geochemical Exploration*, v. 108, p. 143–156.

